Acta Geotechnica (2015) 10:375–387
DOI 10.1007/s11440-014-0353-9

Primary fabric fraction analysis of granular soils

Huu Duc To · Sergio Andres Galindo Torres · Alexander Scheuermann

Received: 1 October 2013 / Accepted: 31 August 2014 / Published online: 17 October 2014

Abstract Granular soil can be considered as a composition of two fractions of particles; an immobile part called the primary fabric, and loose particles located in the voids formed by the immobile part considered to be potentially mobile. The primary fabric transfers momentum through force chains formed by interconnected force chains. These force chains form pores where loose particles are located. As a consequence, loose particles can be mobilised very easily under the influence of seepage flow and transported away if the geometrical conditions of the pore structure allows it. Therefore, the determination of the primary fabric fraction, as well as loose particle fraction, is of vital importance especially in soil suffusion predictions, which must be thoroughly considered in the design of hydraulic structures or their risk assessment. This paper presents a new method to simulate the behaviour of soils under stress and introduces a numerical analysis to define the primary fabric fraction. To achieve this, soil specimens are built by a new sequential packing method, which employs trilateration equations for packing. Later, specimens are compacted under oedometric conditions using the discrete element method to observe how the loading force is distributed across the solid matrix and to identify the fraction of the soil sustaining the external force. The primary fabric fraction analysis is conducted on two types of soil particle arrangements with several grain size distributions. A striking finding of this study is that the portion of the soil belonging to the primary fabric greatly depends on the structural packing of the granular particles. This finding should be used as evidence for the formulation of more accurate criteria for the prediction of suffusion and erosion in the future.

Keywords Discrete element · Force chain · Internal stability · Primary fabric size · Sequential packing · Suffusion

H. D. To (✉)
Geotechnical Engineering Centre, School of Civil Engineering, The University of Queensland, Brisbane, QLD 4072, Australia
e-mail: h.to@uq.edu.au

S. A. Galindo Torres · A. Scheuermann
Geotechnical Engineering Centre, School of Civil Engineering, Research Group on Complex Processes in Geo-Systems, The University of Queensland, Brisbane, QLD 4072, Australia

1 Introduction

Suffusion is commonly acknowledged as one of the main reasons for the internal instability of water retaining structures built with, or founded on, soils [9]. This phenomenon occurs when fine soil particles are dislodged by the seepage flow and transported through series of pore throats called constrictions, which are the narrowest openings along paths connecting pores [17]. Because of the load transfer, coarse particles are initially held firmly in their position. Contrariwise, there are also loose particles within the structure which are not held by force and, as a consequence, are not held in their position. These particles can easily be transported away at some hydraulic gradient [30]. The removal may lead to an increase in the soil porosity and in the hydraulic conductivity as well. At a critical value of the porosity, the firmly held particles may collapse on the micro-scale, forming a new structure with changed constriction sizes. On the macro-scale, the accumulation of these micro-scale changes may lead to some larger pores which enable the movement of even larger loose particles. This internal process becomes visible on the surface of earth structures when soil particles are

washed out with the water outflow, which is final proof of what is commonly denoted as internal instability.

During the last few decades, many experimental studies, aimed at the investigation of suffusion, used soil particle size distribution (PSD) as the basis for a definition of a geometrical criterion in soil internal stability assessment [5, 17, 34]. In these studies, the PSD was used as a proxy for the pore size distribution—or more correctly, pore constriction size distribution (CSD) which is, from the geometrical point of view, the key factor determining whether a particle can be moved out of a porous structure or not. Thus, some researchers suggested a direct comparison between the PSD and the CSD of a soil for the assessment of suffusion [15, 16, 19, 27]. A review and comparison of different methods on how to calculate a CSD from a PSD can be found in Sjah and Vincens's paper [29, 33].

For soil suffusion analysis, the PSD is usually divided in two fractions: (1) a fraction of particles taking over the externally applied stress and forming the primary fabric of the soil, which is referred to as primary fabric fraction in this paper, and (2) another fraction not contributing in this stress transfer considered to be loosely embedded in the pores formed by the primary fabric (Fig. 1), which is denoted as loose fraction in this paper. This consideration of two fractions implies a critical assumption, which is used in many existing suffusion criteria and which in the past was rarely scrutinised and/or seriously discussed in detail, namely, whether there is actually a sharp transition in the PSD, characterised by a particle size threshold, dividing the whole soil into the primary fabric and the loose particles. Although the importance of this assumption seems to be clear, there are no standardised procedures available for defining those fractions. A generally accepted hypothesis assumes that there is an exact particle size dividing the PSD into primary fabric and loose fractions. All soil particles smaller than that particular size belong to the loose fabric fraction, and all larger particles to the primary fabric fraction. This size threshold is usually called the primary fabric size, but can also be found under other names [14, 25]. In an empirical approach, primary fabric size is suggested to be determined by the void ratio of the primary fabric

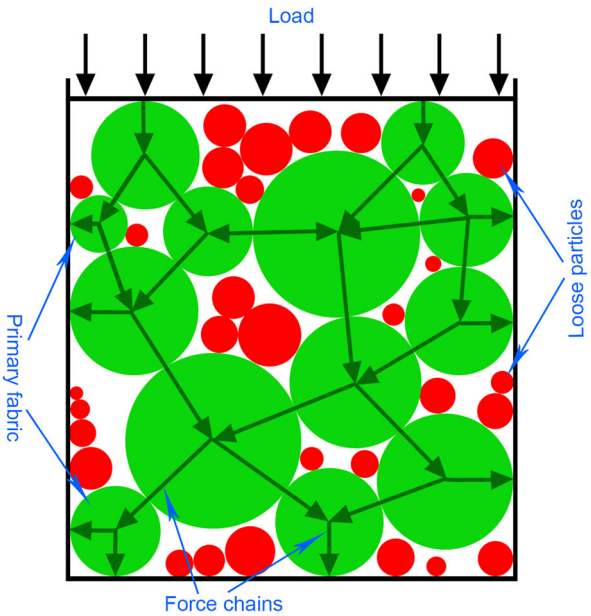

Fig. 1 Primary fabric with contact forces and loose particles as a two-dimensional illustration of a particle package

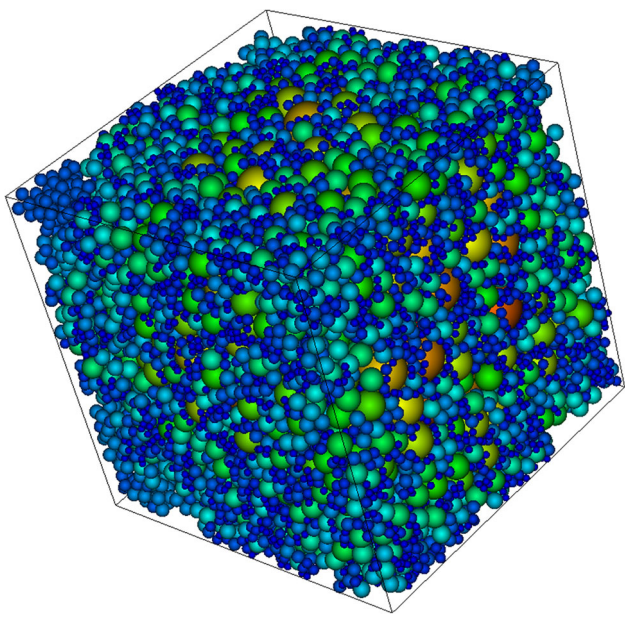

Fig. 2 Discrete arrangement for a PSD with coefficient of uniformity, $C_u = 2.5$ (see Fig. 5)

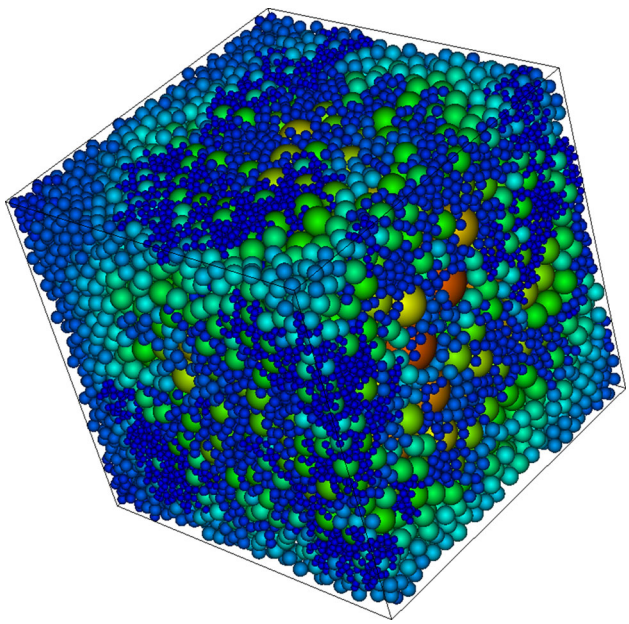

Fig. 3 Layer-wise arrangement for a PSD with coefficient of uniformity, $C_u = 2.5$ (see Fig. 5)

fraction and the average porosity of the loose particle fraction [14, 17]. However, the determination of these values is unclear because it returns to the initial problem: how to determine primary fabric and loose fractions? In addition, the soil fraction forming the primary fabric might vary with the same PSD and porosity, caused by different structural arrangements of the soil particles. The evidence of this hypothesis is given in the primary fabric fraction analysis below.

According to a recent numerical study carried out by the authors, an exact primary fabric size might not exist [31]. There is usually an overlapping zone (OZ) in the PSD, where some particles take part in the primary fabric, while other particles with the same radii are considered to be loose particles. This paper contributes a further study on the surveyed phenomenon, based on computational simulations with several PSDs and two critical types of particle arrangements: discrete arrangement (DA), where fine particles are put between coarser particles leading to a rather homogeneous structure of the particles (Fig. 2), and layer-wise arrangement, where particles with similar radii have priority to be placed next to each other (Fig. 3). The layer-wise arrangement has practical meaning because it simulates soil dumped from trucks at construction sites or the soil restructured by seepage flow. In the case of dumped soil, the larger and heavier particles are dropped down first and accumulate at the toe of a pile, while the fine particles take more time to settle down. In the filtration case, fine particles dislodged by seepage force might block pore throats or constrictions, especially at the interface to another soil body. These processes lead to the assembly of particles with similar sizes.

This paper will illustrate the influence of the PSD and structural particle arrangement on the primary fabric fraction. It will also provide new insight into the formation of particle contacts under loading force to obtain a better understanding of the primary fabrics' behaviour. The test results will be analysed and discussed against the background of suffusion. The specimen is generated by a recent approach in sequential particle packing, while the compaction test is conducted by discrete element method (DEM).

2 Numerical simulation

2.1 General approach

The core step of the simulation procedure employs the sequential packing method [31], which places particles into

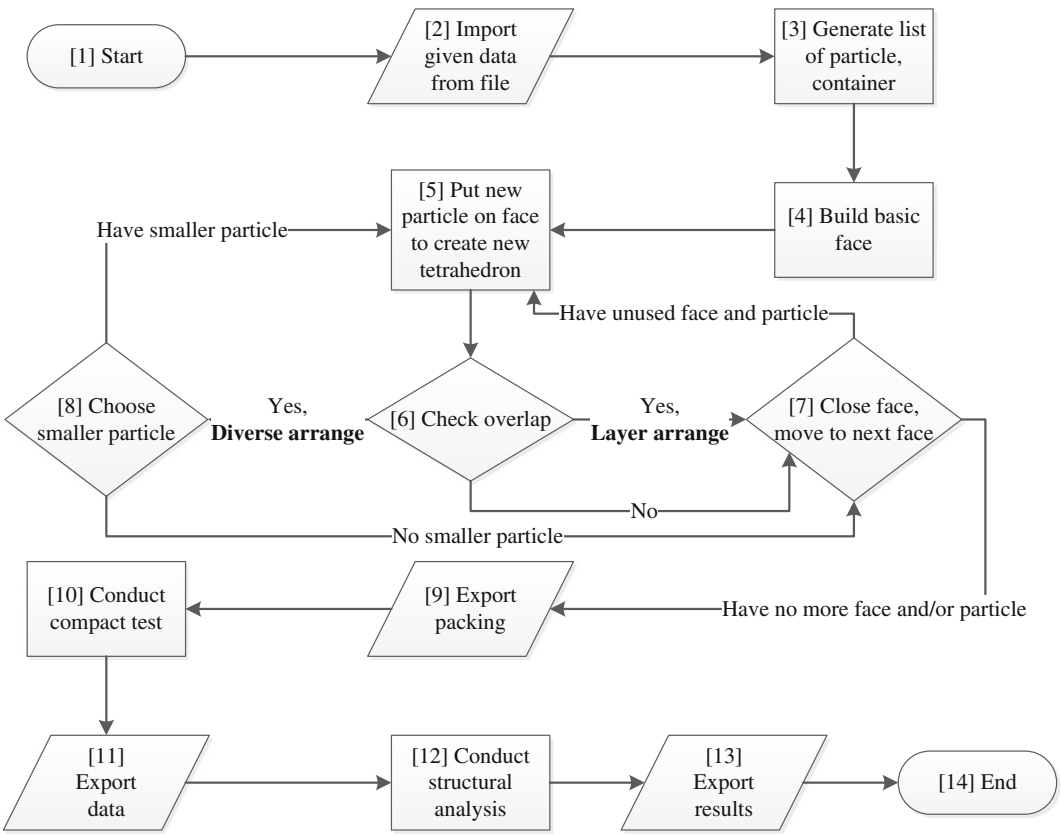

Fig. 4 Main algorithm of the simulation procedure including sequential packing procedure, DEM calculations and analysis of particle structure

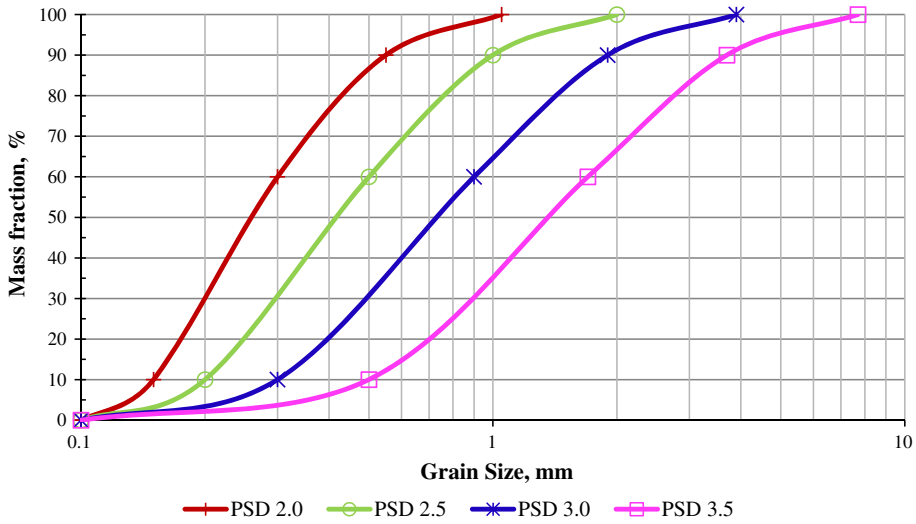

Fig. 5 Particle size distributions with different coefficients of uniformity, $C_u = 2.0, 2.5, 3.0, 3.5$

a virtual container in a predefined sequence, to obtain a packing of spheres with a given PSD and porosity in a pre-calculated volume that is able to accommodate approximately 22,000 to 76,000 particles. Depending on the uniformity of the PSD, more or less particles are needed to fill a given volume satisfying the characteristics of the PSD. The merit of the sequential method against many other packing methods [24, 28] is its ability to simulate particle arrangements [31]. In addition, the simulation takes only a few minutes for the packing process because this method is semi-analytical. In contrast, other models employing DEM need several days for the calculation [24, 28] because its packing process is time-consuming. The simulation code is programmed in C++ using *Mechsys*—a multi-physics computing library developed at The University of Queensland [21]. The sequential packing method presented in this paper was modified from that previously presented in [31].

The arrangement of particles as a result of the sequential packing method is then imported into a DEM model. The criterion for the determination of primary fabric is the support of an externally applied load by individual particles (Fig. 1). In order to simplify the identification of the particles taking on the loads, all particles are set free of gravity. Hence, loose particles will not apply any force due to their weight on other particles underneath. If particles experience force, it must be caused by the externally applied load.

For simplification, in this study, only spheres are used to represent soil particles as this assumption is accepted for the investigation of processes on the pore-scale and justified for generally spherically shaped sandy soils. Although there are several—in some cases very sophisticated—methods available to generate particles with other shapes [4, 11, 22], the spherical shape is still commonly used in most numerical models dealing with soil particle structure

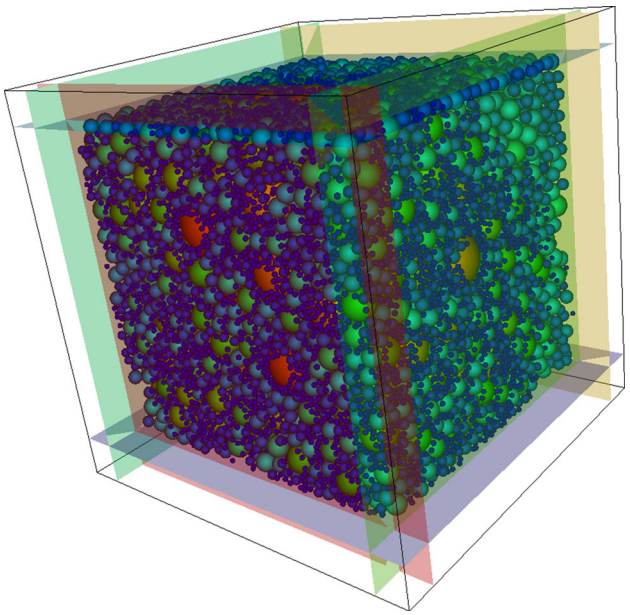

Fig. 6 Particle arrangement imported into cubic container of the DEM model for compaction test

[23, 26, 28], because of its simplicity and applicability for the calculation of an enormous number of particles.

The simulation program employs four PSDs (Fig. 5) with uniformity coefficients, C_u, of 2.0, 2.5, 3.0, and 3.5 and a cubic container (Fig. 6) which has to be filled during the packing process. The soils with $C_u \geq 3.0$ can be considered as wide-graded soils according to Kenney and Lau [17].

2.2 The main algorithm

The simulation's algorithm is shown in Fig. 4, and the details of each individual step are described below:

- The soil parameters, including PSD, porosity, density, soil volume, and shape of specimens, are imported from an input text file (step 2).
- From the data input in step 2, a list of soil particles and a container are generated (step 3). To achieve this, the soil PSD is divided into several intervals, up to 100, represented by a mean diameter. In the current simulation, all PSDs are divided by 5 % of soil mass into 20 intervals. This approach does not change the main form of the soil PSD, but it decreases the ratio between largest and smallest sizes of particles to some extent. The number of particles for each interval is determined by the mean diameter, the given volume and the chosen porosity.
- Three particles are placed into the centre of the container first. They form a triangular face, defined by the coordinates of the particle centres (step 4). To avoid the lack of space for coarse particles at the end of the packing process, the first particle to be placed is the largest.
- A new particle is then attached to the triangular face (step 5) by solving the trilateration Eq. (1) in the local coordinate system. The trilateration equation is usually used in Global Positioning Systems to determine coordinates of an object, when the distances between object and satellites are known.
- After this, the overlap between the added particle and existing particles, including the container, is checked (step 6). If there is no overlap, the face is marked as "closed" (step 7) so that no other particles can be attached to it later. Equally, the particle attached to the face is also marked as "used" in the computational memory to avoid duplicated use. The process of attaching particles repeats continuously with other faces, including the three new faces formed by the latest attached particle, until the point when all particles are depleted or all faces are closed.
- If an overlap occurs (step 6), there are two different treatments depending on the intended structure, such that: (1) in simulations with layer-wise arrangement the face is marked as closed (step 7) because this can help to use particles by descending order of size; and (2) in simulations with DA, another smaller particle will be selected to attach on the face (step 8). Obviously, this approach leads to particle arrangements with different sizes of neighbouring particles. If there is no smaller particle to be chosen, the face is marked as "closed" (step 7).
- After the generation of the total packing, the result is saved (step 9) to be used for the compaction test with DEM (step 10). Because gravity is not imposed in the simulation, loose particles can be placed in space without having any contact with other particles or the container, which simplifies the identification of the primary fabric fraction. The result of the compaction test is saved to be used for the later primary fabric fraction analysis (step 12).

2.3 The sequential packing

Usually, sequential packing methods work in a way where particles can be added sequentially by dropping or rolling them in a container to obtain a stable position [1, 3] or placing them in pores between existing particles [18]. In step 5 of the algorithm presented in this paper, a particle is sequentially placed on a face formed by three existing particles after solving the trilateration Eq. (1) in a local coordinate system. That means that this method controls the structural composition of the packing, whereas in most other packing procedures, the placement of a particle is rather the result of a random process.

$$\begin{cases} x_4^2 + y_4^2 + z_4^2 = (r_1 + r_4)^2 \\ (x_4 - x_2)^2 + y_4^2 + z_4^2 = (r_2 + r_4)^2 \\ (x_4 - x_3)^2 + (y_4 - y_3)^2 + z_4^2 = (r_3 + r_4)^2 \end{cases} \quad (1)$$

where x_i, y_i, z_i, r_i—local coordinates and radii of particle i, respectively.

Equation (1) must be used with a local coordinate system to avoid a case with "division by zero", which can occur when the global coordinate system is used and two of the existing particles are aligned with any axis. The direct analytical solution of Eq. (1) significantly reduces the calculation time since added particles do not need time to find a stable position in the structure as required in other sequential packing methods.

If the added particle is significantly smaller than the constriction size, Eq. (1) does not provide a solution. In this case, if the face is virtually an equal-sided triangle, the new particle will be placed at the centre of the constriction (Fig. 7). Otherwise, the new particle will be placed close to the two larger particles of the existing triple face in DAs or close to the two smaller particles in layer-wise arrangements (Fig. 8). The constriction size is determined by:

$$\begin{cases} x_c^2 + y_c^2 = (r_1 + r_c)^2 \\ (x_c - x_2)^2 + y_c^2 = (r_2 + r_c)^2 \\ (x_c - x_3)^2 + (y_c - y_3)^2 = (r_3 + r_c)^2 \end{cases} \quad (2)$$

where x_c, y_c, r_c—local coordinates and radius of constriction.

In general, when a particle can be placed into a pore or into a constriction, the new particle must be much smaller than the existing particles, except in the case of obtuse triangular faces. Therefore, the second loop in the new sequential method presented here [32] is not employed for layer-wise arrangements in order to make the effect of the

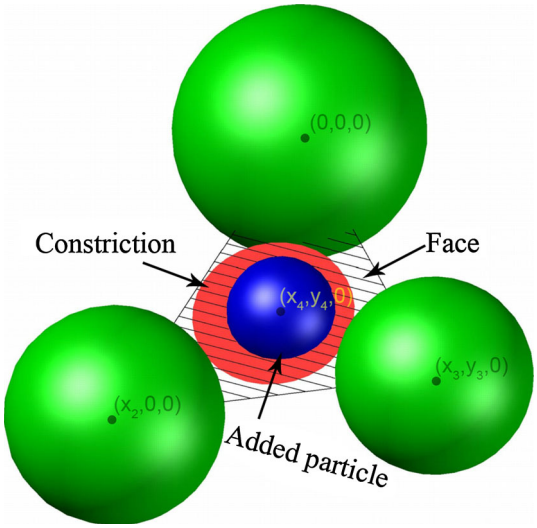

Fig. 7 Central placement of a new particle into the face spanned between the centroids of three existing particles. The coordinates of the centroids are given in the local coordinate system. The diameter of the added particle should be smaller than the diameter of the constriction constructed on the face of the particle assembly

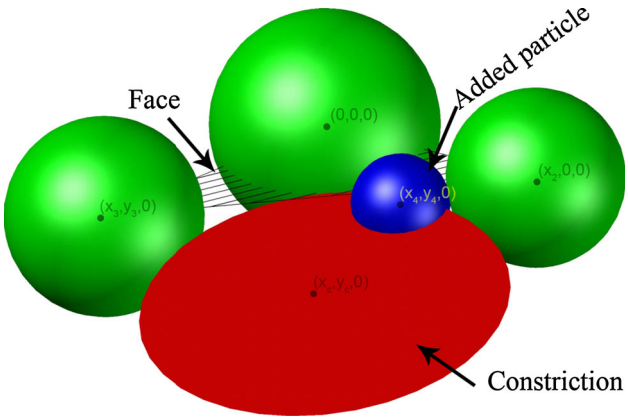

Fig. 8 Adjusted particle touching two existing particles. The coordinates of the centroids are given in the local coordinate system

layer-wise structure more significant. As a consequence, the range of adjustable soil porosities reduces to 0.33–0.38. The influence of porosity on the formation of a primary fabric is not studied in this paper, and the common porosity for all generated soil specimens is given as 0.35.

2.4 The compaction test in DEM

DEM is widely acknowledged as a suitable method in computational simulations of the particle scale. The method divides the time flow by a finite time step, dt. The position of discrete elements in the next time step is calculated from the position, velocity, contact force, and other parameters of the model in the current time step [7]. To achieve this, the contacts between discrete particles can be simulated by beams or strings for cohesive and general materials, respectively [8]. The calculations in this study can draw significant advantage from the geometrical simplicity of the spheres, used as the shape for the particles, by employing some simpler formulas [6, 13] describing the interaction of the particles. Hence, the normal contact force, $\boldsymbol{F}_\mathrm{n}$, by normal direction, $\hat{\boldsymbol{n}}$ can be estimated as:

$$\boldsymbol{F}_\mathbf{n} = K_\mathrm{n}\delta\hat{\boldsymbol{n}} \tag{3}$$

where K_n—normal stiffness, δ—overlapping length.

The tangential force, $\boldsymbol{F}_\mathbf{t}$, is bounded by the Coulomb limit [12] and is estimated as:

$$\boldsymbol{F}_\mathbf{t} = \min(K_\mathrm{t}\delta_\mathrm{t}, \mu F_\mathrm{n})\hat{\boldsymbol{t}} \tag{4}$$

where K_t—tangential stiffness, δ_t—tangential displacement [20], μ—friction coefficient, and $\hat{\boldsymbol{t}} = \boldsymbol{v}_\mathbf{t}/v_\mathrm{t}$ with $\boldsymbol{v}_\mathbf{t}$—tangential velocity.

The viscous force, $\boldsymbol{F}_\mathbf{v}$, is added to dissipate the energy and simulate the inelastic collisions [13]:

$$\boldsymbol{F}_\mathbf{v} = G_\mathrm{n} m_\mathrm{e} v_\mathrm{n}\hat{\boldsymbol{n}} + G_\mathrm{t} m_\mathrm{e} v_\mathrm{t}\hat{\boldsymbol{t}} \tag{5}$$

where G_n, G_t—normal and tangential dissipation constants respectively, m_e—effective mass of the colliding particle pair, $\boldsymbol{v}_\mathbf{n}$—normal velocity.

To simulate the roughness of particles, Mechsys employs a rolling stiffness, β, which is calculated from the tangential stiffness [2]. This method avoids the rolling of spherical particles with high angular velocity at one position. The parameters used in the presented DEM simulations in Mechsys are shown in Table 1 and include values from several other former studies [10, 12]. The simulation produces intermediate output with position and contacts of all soil particles for every time step, and the process ends if the calculating time exceeds the final time, t_f. To avoid the case when the packing has stabilised before t_f is reached, a finite small threshold of the sum of kinetic energy, K, is applied. The calculation stops if the total kinetic energy of all particles in the specimen is smaller than K. Details on the applied DEM model can be found in Galindo-Torres et al.'s paper [13].

The compaction test aims to determine the load transfer through the packing via the particle contacts. Because of the sequential method used, all particles have contacts with at least three other particles and/or the container before the compaction test. The particle contacts and contact forces are visualised by tubes connecting the particle centres (Fig. 9). The length of the tube shows the distance between the particle centres, the thickness and colour display the value of the contact force. In the initial state, tube diameters and colours are the same throughout the packing because neither gravity nor a loading force has been

Table 1 Parameters used for the implementation of DEM calculations

Parameters	Value	Unit
Normal stiffness, K_n	$2.0 \cdot 10^7$	N/m
Tangential stiffness, K_t	$2.0 \cdot 10^7$	N/m
Normal viscous coefficient, G_n	$1.6 \cdot 10^4$	s^{-1}
Tangential viscous coefficient, G_t	$0.8 \cdot 10^4$	s^{-1}
Time step, dt	$31.6 \cdot 10^{-5}$	s
Intermediate output time, d_{tout}	31.6	s
Total time of simulation, t_f	$12.6 \cdot 10^2$	s
Limit kinetic energy, K	10^{-7}	Nm
Rolling stiffness coefficient, β	0.12	
Plastic moment coefficient, η	1.0	

applied. The bottom lid of the container applies an upwards directed stress on the packing which is distributed internally by the primary fabric. Particles with contacts in alignment with the stress direction experience larger contact forces (Fig. 10). The particles contributing to the stress transfer are kept firmly in their place by the contact forces and form force chains. Meanwhile, because of the applied zero gravity, the loose particles are pushed out of the primary fabric by the normal contact force acting between particles. Since these particles tend to have no contacts with other particles, they are removed from the contact illustration (Fig. 10), which supports the identification of the loose particle fraction and the primary fabric fraction. The absence of gravity is a tremendous help in separating the loose fraction and the primary fabric fraction in soils.

3 Results and discussion

3.1 Force chain stability analysis

The force chain stability analysis is conducted to provide a better understanding of the soil's primary fabric behaviour under externally applied loads. It also tries to illustrate the influence of particle arrangements and PSD on the constitution of a primary fabric. To achieve this, the temporal evolution of the force chains after application of the load will be analysed and the magnitude and direction of the created contact forces will be discussed as follows.

From the beginning of the loading test, loose particles already exist since all particles with less than three contacts are considered as loose (Fig. 11). The number of loose particles, initially under 20 %, increases abruptly and reaches a peak during the first time steps after application of the external load. In the case of narrow-graded soils ($C_u = 2.0$ and $C_u = 2.5$), regardless of the particle arrangement, the number of loose particles decreases with time after reaching a peak before it levels off in a stable state. This observation means that with ongoing deformation loose particles are pushed out of the force chains after they have been created. The fluctuation in number and mass of loose particles shows that soil specimens are continuously restructured under load to reach a stable state (Figs. 11, 12). For wide-graded soils ($C_u = 3.0$ and $C_u = 3.5$) in both arrangements, the number of loose particles levels at the peak value or even slightly increases. In the case of soils with $C_u = 3.5$, more than 97 % of the

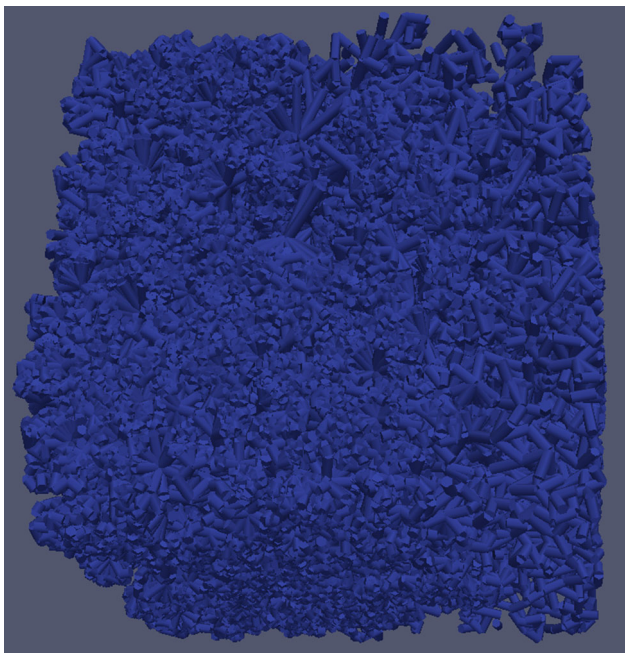

Fig. 9 Particle contacts without loading force ($C_u = 3.5$)

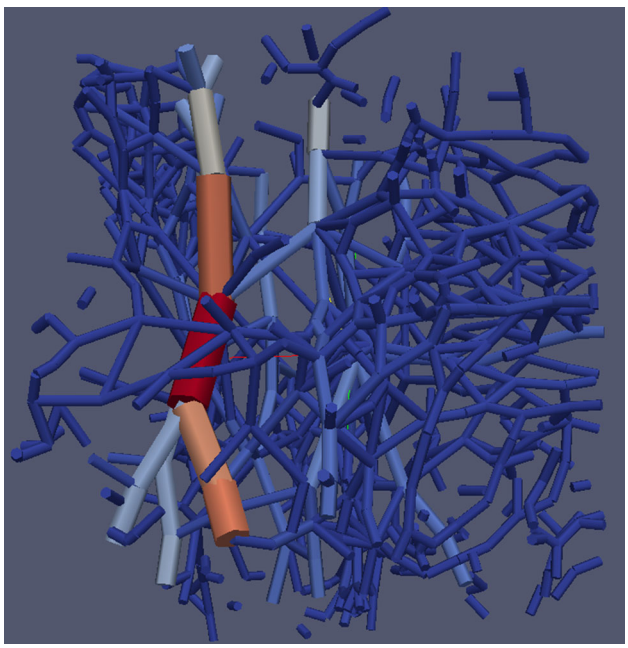

Fig. 10 Particle contacts under loading force ($C_u = 3.5$)

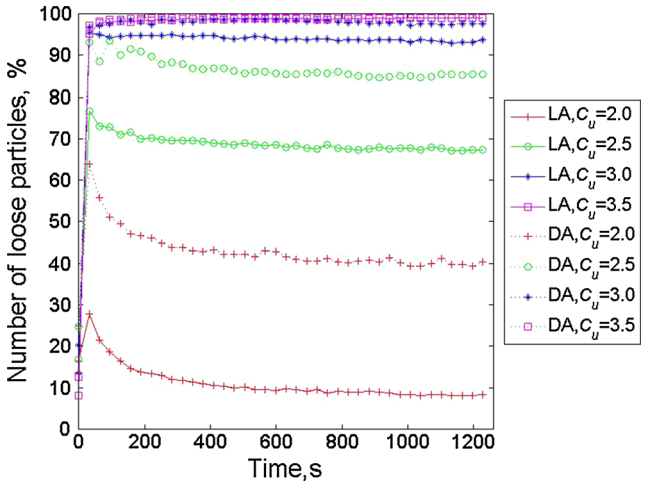

Fig. 11 Percentage of loose particles by number of particles in layer-wise arrangement (LA) and discrete arrangement (DA) for different coefficients of uniformity C_u

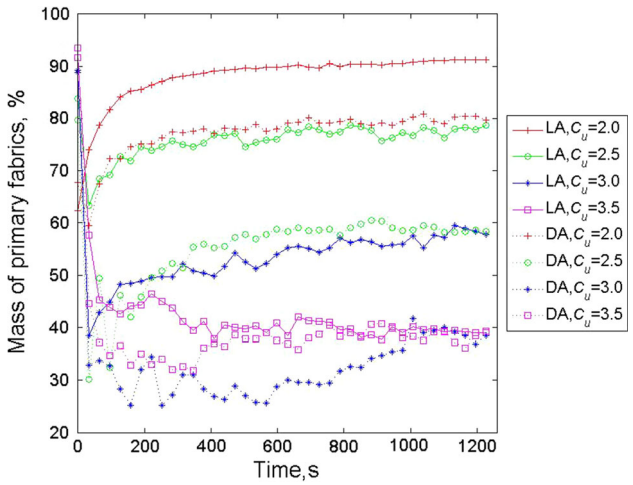

Fig. 12 Percentage of primary fabric fraction by mass comparing layer-wise arrangement (LA) with discrete arrangement (DA) for different coefficients of uniformity C_u

particles in terms of numbers are loose particles and there are only a few particles transferring the load (Fig. 11).

The temporal evolution of the soil mass included in the primary fabric (Fig. 12) shows a naturally reciprocal evolution compared to the temporal changes in the number of loose particles as shown in Fig. 11. Although when $C_u = 3.5$, more than 97 % of the particles by number are considered to be loose particles, at least 40 % by mass belongs to the primary fabric (Fig. 12). The same applies for $C_u = 3.0$ in DA. In the case of soils with $C_u = 3.0$ and layer-wise arrangement, 50 % of the soil mass forms the primary fabric, while 90 % in terms of number of particles is considered to be loose. Generally in all observed cases, the primary fabric fraction takes more mass in layer-wise arrangements than in DAs. It is clear that with the same

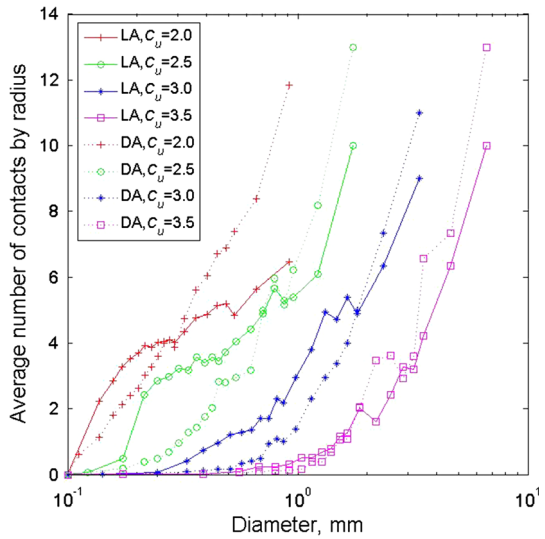

Fig. 13 Average number of contacts per particle in layer-wise arrangement (LA) and discrete arrangement (DA) for different coefficients of uniformity C_u

PSD, the soil specimen with layer-wise arrangement involves more particles in its force chains because the local PSD is often narrower than the global PSD. Meanwhile, the local PSD in DAs tends to have a gap-grade form, which results in more particles free of load. Another important result drawn from this analysis is that the number of particles involved in the force chains in layer-wise arrangements is, in most cases, higher than in DAs.

It is evident that a large particle creates more contacts in a DA (where neighbouring particles can be of every size) than in a layer-wise arrangement (where the sizes of neighbouring particles can be very similar, see Fig. 13). Generally speaking, the more contacts a particle has, the more stable it is. As a consequence, for a given PSD, a packing with DA would be more prone to suffusion just because of the lower average number of contacts per each small particle (Fig. 13). In contrast, the soil with layer-wise arrangement and $C_u = 2.0$ is less prone to suffusion because the fine fraction shows a comparably high average number of contacts.

In general, large particles with more contacts are taking on more contact forces, which means their contribution is the highest in the stress transfer. However, not all of these contacts are firmly fixed especially in DAs. These loose contacts, which mean contacts with small forces, reduce the average force per contact. For the largest particles in soils with $C_u \geq 2.5$, the average contact force is always higher for layer-wise arrangements than for DAs (Fig. 14). This observation encourages the assumption that force chains in DAs might be easier to be restructured.

In order to detach one fine particle from a force chain, the seepage force, which is in many cases predominantly

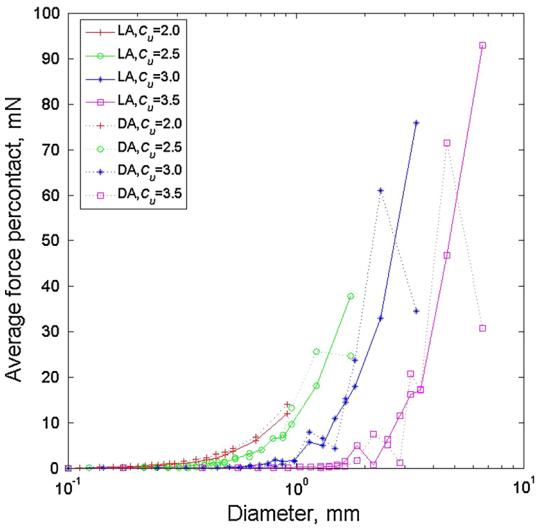

Fig. 14 Average normal force per contact in layer-wise arrangement (LA) and discrete arrangement (DA) for different coefficients of uniformity C_u

horizontally directed, must overcome the resistance created by the contacts with neighbouring particles consisting of both tangential friction and geometrical resistance forces. For instance, in vertical loading, wide-graded soils have a preferred orientation of the forces in a vertical direction, independent of the structural arrangement (Fig. 15) with larger average force values (Fig. 16). Therefore, the force chains in these soils create higher tangential friction forces to keep particles in place. However, these force chains lack in terms of geometrical resistance because of the smaller number of contacts perpendicular to the main direction of stress transfer compared with a more equally distributed direction of forces as in narrow-graded soils ($C_u = 2.0$ and $C_u = 2.5$) (Fig. 15).

In terms of soil structure, the DA creates less horizontal contacts in comparison with layer-wise arrangements (Fig. 15) and these contacts seem to be relatively weaker (Fig. 16). This observation encourages another assumption that the DA creates force chains which are less stable than the force chains produced by layer-wise arrangement because it has less horizontal support in both contact number and contact force. Actually, this discrepancy between these two arrangements seems to increase with increasing C_u (Figs. 15, 16).

It is difficult to assess whether tangential friction or geometrical resistance has more influence on the stability of force chains. However, at least for spherical particles, the force chain network in wide-graded soils seems to be less stable than in narrow-graded soils. This conclusion is supported by the observation that the mass of primary fabric in wide-graded soils fluctuates widely for a long time because the force chains network continuously restructures in order to find a more stable state (Fig. 12).

3.2 Primary fabric fraction analysis

The commonly accepted assumption regarding the identification of the primary fabric of a granular soil is the existence of a sharp delimitation point, which divides the PSD into primary fabric and loose particle fractions. One main objective of this paper is the analysis of the primary fabric, which is advanced to prove the existence of an OZ between the primary fabric fraction and the loose particle fraction in terms of their particle size. This hypothesis contradicts the assumption introduced before with crucial consequences regarding suffusion analysis.

It seems that for soils with small C_u the OZ might be notably large because of the small variation in particle sizes, which is the case for $C_u = 2.0$ and layer-wise arrangement as shown in Fig. 17 where the original PSD and the distribution of the primary fabric almost matches. For the same PSD and DA, this OZ reduces.

For a larger C_u, the gap increases between PSD and the primary fabric and loose particle fractions, irrespective of the arrangement used (Figs. 17, 18). Visually, there does not seem a huge difference in the shape of the distributions of primary fabric and loose particle fractions and the PSD for the different arrangements. In fact, for given PSDs, the particle sizes over which the OZ spans do not change much for the different arrangements, and the percentage of the soil mass included in the OZ changes very little if at all (Table 2). Except in the case of $C_u = 2.0$ and layer-wise arrangement, the OZ takes about 85 % of soil mass. This OZ remains 70 % for all other layer-wise arrangements. A marginal decreasing trend can be seen from 75 to 65 % in samples with DA. It is reasonable to assume that with increasing C_u this OZ becomes smaller relative to the overall span of the PSD. However, it is justified to assume that an OZ always exists also in well-graded granular soils.

The question remaining about the size fractions included in the primary fabric is answered in Fig. 19. As can be seen for a sample with $C_u = 2.0$ and layer-wise arrangement, more than 80 % of the mass of the finest fraction is considered to be included in the primary fabric. This number decreases notably for $C_u = 2.0$ with a DA and for all other samples with higher C_u values. Naturally, the percentage of mass included in the primary fabric for each interval increases with increasing particle size. An interesting observation from Fig. 19 is that regardless of the uniformity of the sample and the chosen arrangement, a fraction of fine particles always seems to be included in the primary fabric. In contrast, with increasing values of C_u, larger particles are increasingly included in the primary fabric until they are all part of the stress transferring fraction of the soil, which seems to be obvious given that the number of contacts on large particles must increase with increasing C_u. For samples with $C_u = 3.5$, already the last two

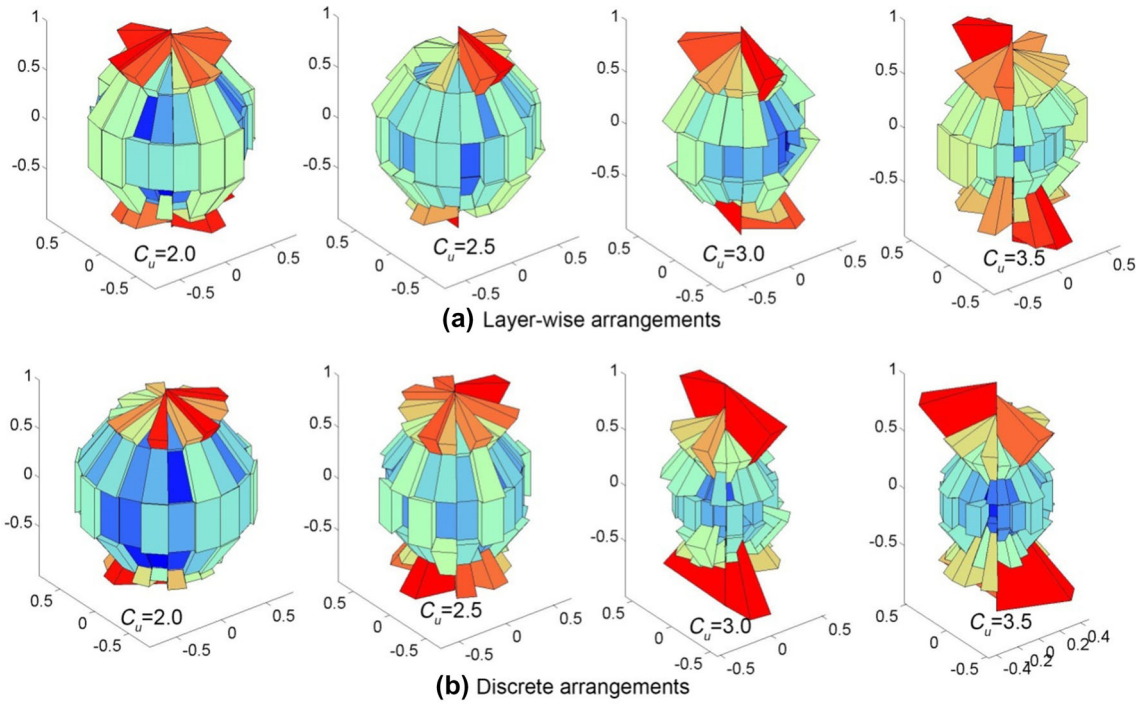

Fig. 15 Spatial distribution of contact direction for **a** layer-wise arrangement, and **b** discrete arrangement for different values of C_u. Note that all data have been normalised, that is, the largest value in the three-dimensional histogram is 1. *Colour* and *size* of wedge shows the number of contacts

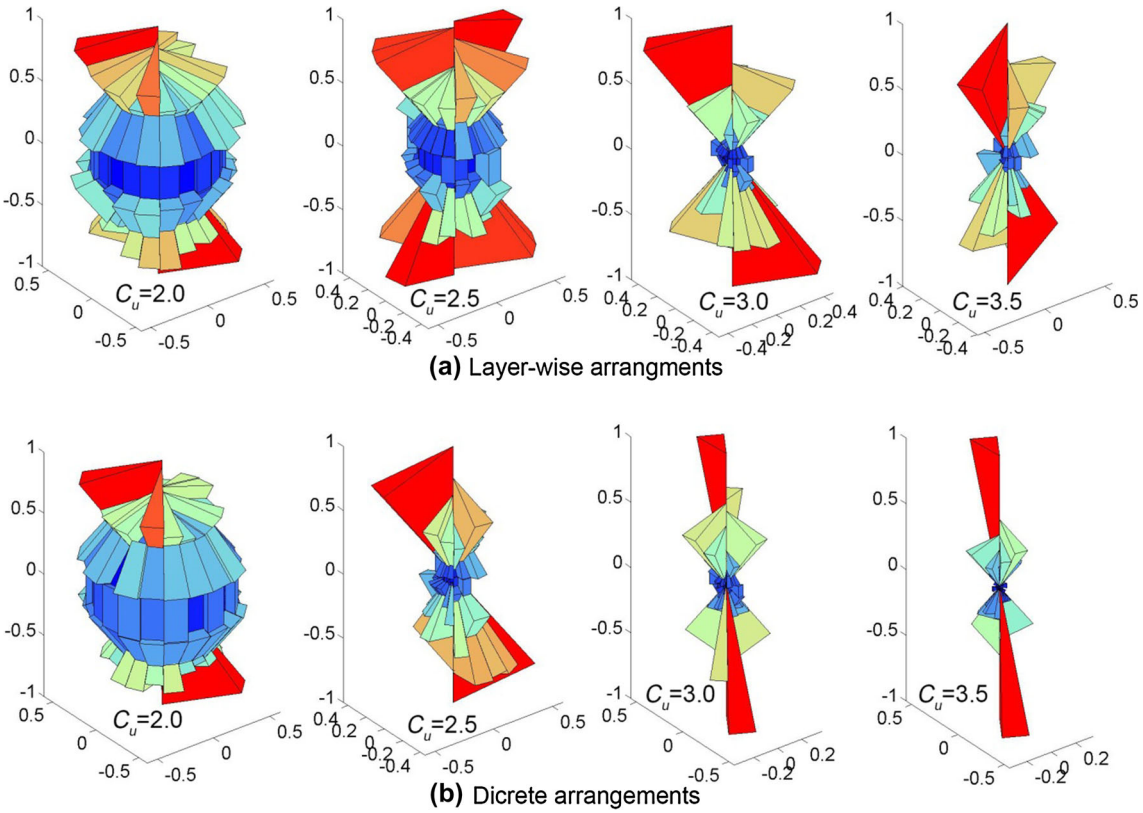

Fig. 16 Spatial distribution of normal contact force for **a** layer-wise arrangement and **b** discrete arrangement for different values for C_u. Note that all data have been normalised, that is, the largest value in the three-dimensional histogram is 1. *Colour* and *size* of wedge shows the number of contacts

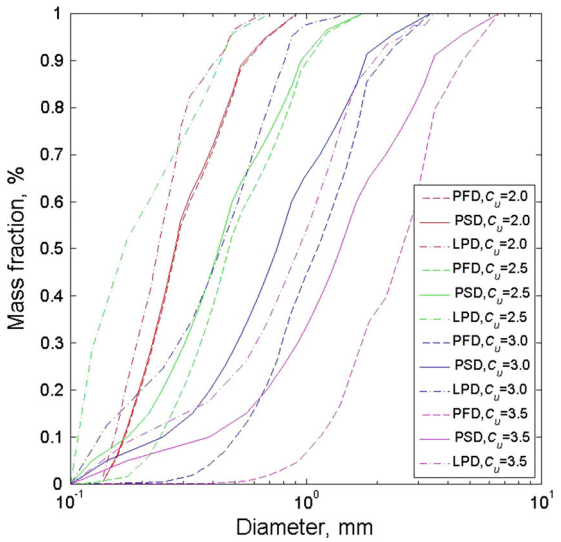

Fig. 17 Primary fabric distribution (PFD), simulated particle size distribution (PSD), and loose particle distribution (LPD) for layer-wise arrangement (LA)

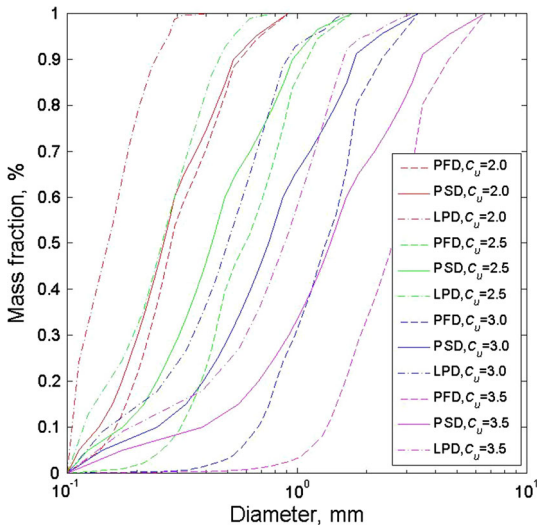

Fig. 18 Primary fabric distribution (PFD), simulated particle size distribution (PSD), and loose particle distribution (LPD) for discrete arrangement (DA)

intervals with the largest particles are 100 % included in the primary fabric.

4 Conclusion

The paper has presented an approach for investigating the primary fabric formation of granular soils by means of DEM calculations. The core of the approach is a novel sequential packing algorithm which allows for the controlled packing of spherical shaped particles in a given cubic volume under controlled porosity and structural arrangement conditions, namely homogeneous (discrete arrangement) or layered (layer-wise arrangement). The particle assembly is then imported into a DEM model to apply vertical loads under zero gravity conditions until equilibrium is reached in terms of the number of mechanically loaded particles. The force chain network of this condition is then analysed against the background of suffusion, quantifying the primary fabric and loose particles fractions, respectively. Samples of four different PSDs and two different particle arrangements (discrete and layer-wise) have been investigated under constant porosity conditions. The main results of this study may be summarised as follows:

- The mass of particles included in the primary fabric fraction varies between 40 and 90 % of the soil mass depending on uniformity of the PSD and particle arrangement. The smaller the uniformity of the PSD, the larger is the mass of soil included in the primary fabric; and for a given PSD, the more homogeneous the structure, the less mass is included in the primary fabric. For high coefficients of uniformity, the influence of the structure on the mass of soil attributed to the primary fabric reduces.
- The stability of force chains is dependent on the particle arrangement. The force chain network in DAs seems to be less stable than in layer-wise arrangements because it involves much fewer particles and force chains. Hence, the fraction of primary fabric in DAs fluctuates more widely in comparison with the primary fabric fraction in layer-wise arrangements.
- The PSD of particles included in the primary fabric and the distribution of particles forming the loose particles fraction have shown an OZ for all samples, which includes 65–85 % of the overall soil mass. This result refutes the hypothesis of an exact primary fabric size in suffusion assessments, at least for PSD and particle arrangements of the tested soils.

The most important outcome of this study is the finding and proof of the existence of an OZ between the PSD of the primary fabric and the loose particles fraction. In existing suffusion analysis methods, a sharp delimitation point is assumed, which divides both fractions. The resulting PSDs are then used for proving the stability against suffusion using simple filtration criteria. It is not clear so far, how large the error might be when this OZ is neglected in suffusion assessment. A new assessment method taking the OZ into account is currently under development.

An interesting observation in terms of the constitution of a primary fabric is that regardless of the PSD and structural arrangement, particles of the fines fraction have always been included in the primary fabric. However, with

Table 2 Overlapping zone analysis for different values of C_u and different structural arrangements. Lower, r_1, and upper bound, r_2, of the overlapping zone, and overlapping zone fraction as percentage of soil mass included in the overlapping zone

Model	Arrangement	C_u	r_1 (mm)	r_2 (mm)	OZ fraction (%)
1	LA	2.0	0.08	0.33	85.00
2	LA	2.5	0.09	0.35	70.00
3	LA	3.0	0.16	0.74	70.00
4	LA	3.5	0.34	1.76	70.00
5	DA	2.0	0.06	0.20	75.00
6	DA	2.5	0.11	0.40	70.00
7	DA	3.0	0.19	0.82	70.00
8	DA	3.5	0.40	1.60	65.00

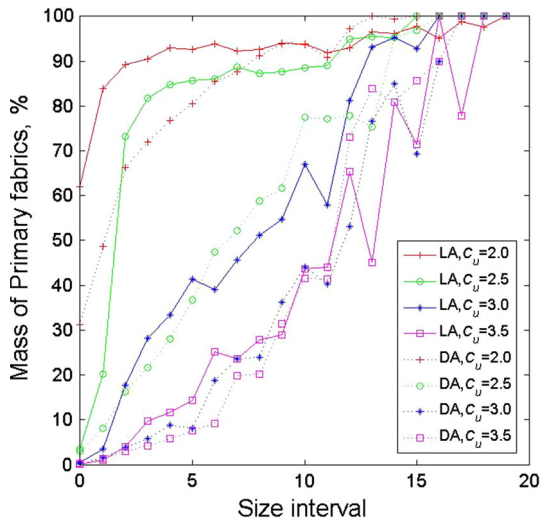

Fig. 19 Contribution of each fraction towards the primary fabric as a percentage of the total mass in each fraction for layer-wise (LA) and discrete (DA) particle arrangements. The PSD is divided into 20 fractions leading to differently sized intervals for different C_u

increasing coefficient of uniformity, particles of the largest fractions were fully included in the primary fabric. The persistence of fine particles in force chains against relocation due to rearrangement of the force chain network is of course questionable, because of the limited number of contacts which keeps them in place. Nevertheless, there seems to be evidence that basically all particle sizes within a PSD contribute to the primary fabric. In this connection, one should keep in mind that all particles are set free of gravity. As a consequence, the resulting force chains can be rearranged much easier than under gravity where body forces from loose particles restrain primary fabric from moving and rearranging.

The introduced method combining a novel sequential packing method with sophisticated DEM calculations seems to be the perfect tool for investigating the mechanical stability of granular packing. The comparison between primary fabric—or more accurately the constriction sizes formed by the primary fabric—and the PSD of the loose particles fraction provides the basis for the potential of suffusion. Although only spherical particles have been considered in the presented research, the results already provide a much improved insight into effects of particle arrangement on the formation of the primary fabric. The next step of this research will be to study the influence of arbitrarily shaped particles on the formation of the primary fabric.

Another interesting question arises that concerns large loose particles, which are not included in the primary fabric, but cannot be removed from pores. Obviously, those particles do not transfer externally applied force, but they still prevent movement of fine particles. A complete answer can be provided only by full suffusion simulation involving seepage flow, which is another focus for future research in this area.

Acknowledgments The first author was granted a scholarship from the Vietnamese Ministry of Education and Training (MOET) and a top-up scholarship from the Graduate School of The University of Queensland (UQ). The presented research is part of the Discovery Project (DP120102188) Hydraulic erosion of granular structures: experiments and computational simulations were funded by the Australian Research Council. The simulations were based on Mechsys, an open source library and carried out using the Macondo Cluster from the School of Civil Engineering at The University of Queensland. The first author also obtained benefit from the GSITA of UQ.

References

1. Bagi K (2005) An algorithm to generate random dense arrangements for discrete element simulations of granular assemblies. Granul Matter 7(1):31–43
2. Belheine N et al (2009) Numerical simulation of drained triaxial test using 3D discrete element modeling. Comput Geotech 36(1):320–331
3. Bezrukov A, Bargieł M, Stoyan D (2002) Statistical analysis of simulated random packings of spheres. Part Part Syst Charact 19(2):111–118
4. Buechler S, Johnson S (2013) Efficient generation of densely packed convex polyhedra for 3D discrete and finite-discrete element methods. Int J Numer Methods Eng 94(1):1–19
5. Burenkova V (1993) Assessment of suffusion in non-cohesive and graded soils. In: Brauns J, Schuler U (eds) Filters in geotechnical and hydraulic engineering. Balkema, Rotterdam
6. Cundall PA, Strack OD (1979) A discrete numerical model for granular assemblies. Geotechnique 29(1):47–65
7. Cundall PA, Strack ODL (1979) Discrete numerical model for granular assemblies. Int J Rock Mech Min Sci Geomech Abstr 16(4):77
8. D'Addetta GA (2004) Discrete models for cohesive frictional materials. D93-Dissertation an der Universität Stuttgart, p 202. ISBN 2-00-014015-8
9. Foster M, Fell R, Spannagle M (2000) The statistics of embankment dam failures and accidents. Can Geotech J 37:25
10. Galindo-Torres S, Muñoz J, Alonso-Marroquin F (2010) Minkowski-Voronoi diagrams as a method to generate random

packings of spheropolygons for the simulation of soils. Phys Rev E 82(5):056713
11. Galindo-Torres S, Pedroso D, Williams D, Li L (2012) Breaking processes in three-dimensional bonded granular materials with general shapes. Comput Phys Commun 183(2):266–277
12. Galindo-Torres S et al (2012) Breaking processes in three-dimensional bonded granular materials with general shapes. Comput Phys Commun 183(2):266–277
13. Galindo-Torres S et al (2013) A micro-mechanical approach for the study of contact erosion. Acta Geotech 1–12. doi:10.1007/s11440-013-0282-z
14. Indraratna B, Nguyen VT, Rujikiatkamjorn C (2011) Assessing the Potential of Internal Erosion and Suffusion of Granular Soils. J Geotech Geoenviron Eng 137:550
15. Indraratna B, Raut AK, Khabbaz H (2007) Constriction-based retention criterion for granular filter design. J Geotech Geoenviron Eng 133(3):266–276
16. Kenney T et al (1985) Controlling constriction sizes of granular filters. Can Geotech J 22(1):32–43
17. Kenney T, Lau D (1985) Internal stability of granular filters. Can Geotech J 22(2):215–225
18. Lind PG, Baram RM, Herrmann HJ (2008) Obtaining the size distribution of fault gouges with polydisperse bearings. Phys Rev E 77(2):021304
19. Locke M, Indraratna B, Adikari G (2001) Time-dependent particle transport through granular filters. J Geotech Geoenviron Eng 127(6):521–529
20. Luding S (2008) Cohesive, frictional powders: contact models for tension. Granul Matter 10(4):235–246
21. Mechsys homepage. Available from: http://mechsys.nongnu.org/index.shtml
22. Oñate E et al (2011) Advances in the particle finite element method (PFEM) for solving coupled problems in engineering. In: Oñate E, Owen R (eds) Particle-based methods. Springer, Berlin, pp 1–49
23. Reboul N, Vincens E, Cambou B (2010) A computational procedure to assess the distribution of constriction sizes for an assembly of spheres. Comput Geotech 37(1):195–206
24. Reboul N, Vincens E, Cambou B (2010) A computational procedure to assess the distribution of constriction sizes for an assembly of spheres. Comput Geotech 37:12
25. Sadaghiani MS, Witt K (2011) Variability of the grain size distribution of a soil related to suffusion. In: Vogt, Schuppener, Straub, Bräu (eds) Paper presented at the 3rd international symposium on geotechnical risk and safety (ISGSR) 2011, Bundesanstalt für Wasserbau. ISBN 978-3-939230-01-4
26. Scholtès L, Hicher P-Y, Sibille L (2010) Multiscale approaches to describe mechanical responses induced by particle removal in granular materials. Comptes Rendus Mécanique 338(10):627–638
27. Sherard JL (1979) Sinkholes in dams of coarse, broadly graded soils. In: 13th congress on large dams. New Delhi, India
28. Shire T, O'Sullivan C (2013) Micromechanical assessment of an internal stability criterion. Acta Geotech 8(1):81–90
29. Sjah J, Vincens E (2011) A comparison of different methods to compute the constriction size distribution for granular filters. In: 13th international conference of the IACMAG. Melbourne
30. Skempton AW, Brogan JM (1994) Experiments on piping in sandy gravels. Géotechnique 44(3):12
31. To HD, Scheuermann A, Williams DJ (2012) A new simple model for the determination of the pore constriction size distribution. In: 6th international conference on scour and erosion. Societe Hydrotechnique de France, Paris, pp 60–68
32. To HD, Scheuermann A, Williams DJ (2012) A new simple model for the determination of the pore constriction size distribution. In: 6th international conference on scour and erosion (ICSE-6). Société Hydrotechnique de France (SHF)
33. Vincens E, Witt KJ, Homberg U (2014) Approaches to determine the constriction size distribution for understanding filtration phenomena in granular materials. Acta Geotech 1–13. doi:10.1007/s11440-014-0308-1
34. Wan CF, Fell R (2008) Assessing the potential of internal instability and suffusion in embankment dams and their foundations. J Geotechn Geoenviron Eng 134:401